

Journal of
Mechanics of
Materials and Structures

**TRANSIENT RESPONSE OF MAGNETO-ELECTRO-ELASTIC
SIMPLY SUPPORTED CYLINDER USING FINITE ELEMENT**

Atul Daga, Natrajan Ganesan and Krishnapillai Shankar

Volume 3, N° 2

February 2008



mathematical sciences publishers

TRANSIENT RESPONSE OF MAGNETO-ELECTRO-ELASTIC SIMPLY SUPPORTED CYLINDER USING FINITE ELEMENT

ATUL DAGA, NATRAJAN GANESAN AND KRISHNAPILLAI SHANKAR

The transient response of a simply supported layered cylinder made of a three-phase magneto-electro-elastic (MEE) composite, consisting of an elastic matrix reinforced with piezoelectric and piezomagnetic fiber has been studied by developing a semianalytical finite element method employing fourth-order Runge–Kutta method. Numerical results are presented for different volume fractions of piezomagnetic fiber in a three-phase MEE material with simply supported boundary conditions. A study of the transient responses of (PZT)-epoxy mixed component (PECP), (Terfenol-D)-epoxy mixed components (MSCP), barium titanate (BaTiO_3) and a two phase magneto-electro-elastic layered cylinder, under simply supported boundary conditions has also been presented. A comparison between the elastic and the coupled responses of the MEE cylinder is presented as well. Ansys 8.1 is used to validate the present code for the response of cylinder made of PECP and MSCP materials.

1. Introduction

The term magneto-electro-elastic solid has been used to refer to a class of materials exhibiting the coupling between mechanical, electric and magnetic fields. Composites made with piezoelectric and piezomagnetic phases not only have the original piezoelectric and piezomagnetic properties but also exhibit magneto-electric coupling effects which are not present in the constituents. Due to the ability of converting one form of energy to another, these materials have a number of applications such as sensors and actuators, in medical ultrasonic imaging, etc. A composite made of piezoelectric and piezomagnetic phases would be susceptible to brittle fracture because these materials are usually brittle ceramics. A three-phase magneto-electro-elastic composite consisting of piezoelectric and piezomagnetic phases separated by a polymer matrix would have greater ductility and formability [Jaesang et al. 2005]. One example of such a material is an elastic matrix made of epoxy reinforced with piezoelectric (BaTiO_3) and piezomagnetic fiber (CoFe_2O_4) fibers.

Due to the simple geometry and wide application, layered cylinder made of magneto-electro-elastic material has been of interest to various researchers. [Pan and Heyliger 2002] obtained the exact solution for three dimensional, linear, anisotropic magneto-electro-elastic and multilayered rectangular plates under simply supported edge conditions. Wang and Zhong [2003] studied the finitely long magneto-electro-elastic circular cylindrical shell under pressure and temperature changes using power series expansion method together with the Fourier series expansion method. Free vibrations studies of the magneto-electro-elastic cylindrical shell have been carried out by various authors [Buchanan 2003; Bhangale and Ganesan 2005; Annigeri et al. 2006]. The transient responses of the inelastic shells of revolution using finite difference solution techniques in time and space has been presented by Philip [1972]. Bhimaraddi

Keywords: magneto-electro-elastic, transient, finite element, Runge–Kutta.

[1987] studied the static and transient responses of composite cylindrical shell based on shear deformation theory using Newmark time integration method. Hou and Leung [2004] studied the transient response of a special nonhomogenous magneto-electro-elastic hollow cylinder using separation of variables and orthogonal expansion method. The plane strain problem is reduced to Volterra integrals, which are solved by means of interpolation method.

In this paper, the transient responses for different volume fractions of the piezomagnetic fiber in a three-phase magneto-electro-elastic layered cylinder under constant internal pressure with simply supported boundary conditions have been studied by developing the semianalytical finite element method using the constitutive equations of the piezomagnetic medium. The fourth-order Runge–Kutta method is employed to obtain the responses. The transient response for (PZT)–epoxy mixed component (PECP), (Terfenol-D)–epoxy mixed components (MSCP), barium titanate (BaTiO₃) and two phase magneto-electro-elastic (MEE) materials is also presented. A comparative study of the elastic and coupled responses of the three-phase MEE layered cylinder has also been done.

2. Constitutive equations

The constitutive equations for the magneto-electro-elastic medium relating stress σ_j , electric displacement D_j and magnetic induction B_j to strain S_k , electric field E_k and magnetic field H_k , exhibiting linear coupling between magnetic, electric and elastic field can be written as [Buchanan 2003]:

$$\sigma_j = C_{jk}S_k - e_{kj}E_k - q_{kj}H_k, \tag{1}$$

$$D_j = e_{jk}S_k + \varepsilon_{jk}E_k + m_{jk}H_k, \tag{2}$$

$$B_j = q_{jk}S_k + m_{jk}E_k + \mu_{jk}H_k, \tag{3}$$

where, C_{jk} , ε_{jk} and μ_{jk} are elastic, dielectric and magnetic permeability coefficients respectively and e_{kj} , q_{jk} and m_{jk} are the piezoelectric, piezomagnetic and magneto-electric material coefficients. The strain displacement, electric field-electric potential and magnetic field-magnetic potential used in finite

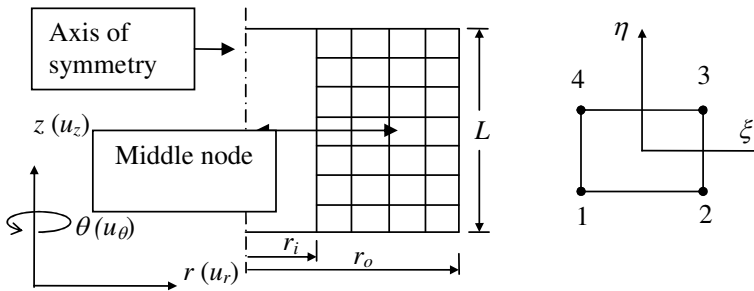


Figure 1. Cylinder discretization with four noded rectangular elements.

element method for the axisymmetric layered cylinder can be written as

$$\begin{aligned} S_{rr} = S_1 = \frac{\partial u}{\partial r}, \quad S_{\theta\theta} = S_2 = \frac{1}{r} \left(\frac{\partial v}{\partial \theta} + u \right), \\ S_{zz} = S_3 = \frac{\partial w}{\partial z}, \quad S_{rz} = S_5 = \frac{\partial w}{\partial r} + \frac{\partial u}{\partial z}, \end{aligned} \tag{4}$$

where u, v and w are the mechanical displacements in the r, θ and z directions. The electric field vector E_i is related to electric potential ϕ as

$$E_r = E_1 = -\frac{\partial \phi}{\partial r}, \quad E_z = E_3 = -\frac{\partial \phi}{\partial z}. \tag{5}$$

Similarly the magnetic field H_i is related to the magnetic potential ψ as

$$H_r = H_1 = -\frac{\partial \psi}{\partial r}, \quad H_z = H_3 = -\frac{\partial \psi}{\partial z}. \tag{6}$$

3. Finite element formulation

The finite element formulation for the axisymmetric layered cylinder with five degrees of freedom per node, u_r, u_z, u_θ, ϕ and ψ , is shown in Figure 1. Since the geometry and material properties of the layered cylinder do not vary along the circumferential θ direction, a simplified solution can be assumed by considering a function in the circumferential direction. The displacement, electric potential and magnetic potential can be written as trigonometric functions in the circumferential direction using the semianalytical finite element as

$$\begin{aligned} u_r = \sum u_r^n \cos n\theta, \quad u_\theta = \sum u_\theta^n \cos n\theta, \\ u_z = \sum u_z^n \cos n\theta, \quad \phi = \sum \phi^n \cos n\theta, \\ \psi = \sum \psi^n \cos n\theta, \end{aligned} \tag{7}$$

where $n = 0$ for axisymmetric case. Due to the orthogonal property of the trigonometric function, the solution becomes decoupled, a fact which leads to substantial saving in computational time. A four-noded rectangular element is used to model the layered cylinder structure.

The mechanical displacements, electrical, and magnetic potential can be expressed as $u = [N_i]\{u\}$, $\phi = [N_i]\{\phi\}$, $\psi = [N_i]\{\psi\}$, with $i = 1, 2, 3, 4$. The formulation for coupled field can be written in terms of the following stiffness matrices [Buchanan 2003]:

$$\begin{aligned} [[K_{uu}] - \omega^2[M]]\{U\} + [K_{u\phi}]\{\phi\} + [K_{u\psi}]\{\psi\} = F(t), \quad [K_{u\phi}]^T\{U\} - [K_{\phi\phi}]\{\phi\} - [K_{\phi\psi}]\{\psi\} = 0, \\ [K_{u\psi}]^T\{U\} - [K_{\phi\psi}]^T\{\phi\} - [K_{\psi\psi}]\{\psi\} = 0, \end{aligned} \tag{8}$$

where $F(t)$ is the constant pressure force as a function of time and

$$\begin{aligned}
 [K_{uu}] &= \int_v [B_u]^T [C] [B_u] dV, & [K_{u\phi}] &= \int_v [B_u]^T [e] [B_\phi] dV, \\
 [K_{u\psi}] &= \int_v [B_u]^T [q] [B_\psi] dV, & [K_{\phi\phi}] &= \int_v [B_\phi]^T [\varepsilon] [B_\phi] dV, \\
 [K_{\psi\psi}] &= \int_v [B_\psi]^T [\mu] [B_\psi] dV, & [K_{\phi\psi}] &= \int_v [B_\phi]^T [m] [B_\psi] dV, \\
 [M] &= \int_v [N]^T [\rho] [N] dV.
 \end{aligned} \tag{9}$$

$[B_u]$, $[B_\phi]$ and $[B_\psi]$ are shape function derivative matrices for strain displacement, electric field-electric potential and magnetic field-magnetic potential, respectively. Here $dV = 2\pi r dr dz$. Electric potential and magnetic potential can be removed from Equations (9) by condensation techniques resulting in

$$[M]\{\ddot{U}\} + [K_{eq}]\{U\} = F(t), \tag{10}$$

where

$$[K_{eq}] = [K_{uu}] + [K_{u\phi}][K_{II}]^{-1}[K_I] + [K_{u\psi}][K_V]^{-1}[K_{IV}]. \tag{11}$$

$[K_{eq}]$ is the equivalent stiffness matrix for magneto-electro-elastic material properties. The component matrices of Equation (11) are

$$\begin{aligned}
 [K_I] &= [K_{u\phi}]^T - [K_{\phi\psi}][K_{\psi\psi}]^{-1}[K_{u\psi}], & [K_{II}] &= [K_{\phi\phi}] - [K_{\phi\psi}][K_{\psi\psi}]^{-1}[K_{\phi\psi}]^T, \\
 [K_{IV}] &= [K_{u\psi}]^T - [K_{\phi\psi}]^T [K_{\phi\phi}]^{-1}[K_{u\phi}]^T, & [K_V] &= [K_{\psi\psi}] - [K_{\phi\psi}]^T [K_{\phi\phi}]^{-1}[K_{\phi\psi}].
 \end{aligned} \tag{12}$$

The eigen vectors corresponding to ϕ and ψ are given by

$$\phi = [K_{II}]^{-1}[K_I]\{U\}, \tag{13}$$

$$\psi = [K_V]^{-1}[K_{IV}]\{U\}. \tag{14}$$

To study the pure piezoelectric effect, the stiffness matrix can be derived as

$$[K_{\phi\phi,eq}] = [K_{uu}] + [K_{u\phi}][K_{\phi\phi}]^{-1}[K_{u\phi}]^T, \tag{15}$$

and to study the pure magnetic effect, the stiffness matrix can be derived as

$$[K_{\psi\psi,eq}] = [K_{uu}] + [K_{u\psi}][K_{\psi\psi}]^{-1}[K_{u\psi}]^T. \tag{16}$$

$[K_{\phi\phi,eq}]$, $[K_{\psi\psi,eq}]$ are the equivalent stiffness matrix considered for studying pure piezoelectric and piezomagnetic cylinder.

4. Results and discussions

4.1. Validation. Ansys 8.1 (www.ansys.com) has been used to validate the code developed for finding the transient response of a magneto-electro-elastic layered cylinder. Ansys cannot directly handle the magneto-electro-elastic material; hence the code has been validated with Ansys 8.1 for the response of

| Materials | PECP | MSCP | MEE | BaTiO ₃ |
|-----------------|-------|-------|-------|--------------------|
| C_{11} | 79.7 | 31.1 | 166 | 166 |
| C_{12} | 35.8 | 15.2 | 77 | 77 |
| C_{13} | 35.8 | 15.2 | 78 | 78 |
| C_{33} | 66.8 | 35.6 | 162 | 162 |
| C_{44} | 17.2 | 13.6 | 43 | 43 |
| e_{15} | 10.5 | 0 | 11.6 | 11.6 |
| e_{31} | -5.9 | 0 | -4.4 | -4.4 |
| e_{33} | 15.2 | 0 | 18.6 | 18.6 |
| ϵ_{11} | 15.92 | 0 | 11.2 | 11.2 |
| ϵ_{33} | 15.92 | 0 | 12.6 | 12.6 |
| μ_{11} | 0 | 0.054 | 0.05 | 0.05 |
| μ_{33} | 0 | 0.054 | 0.1 | 0.1 |
| q_{15} | 0 | -60.9 | 550 | 0 |
| q_{31} | 0 | 156.8 | 580.3 | 0 |
| q_{33} | 0 | 108.3 | 699.7 | 0 |
| m_{11} | 0 | 0 | 5 | 0 |
| m_{33} | 0 | 0 | 3 | 0 |

Table 1. Material properties for (PZT)-epoxy mixed component (PECP), (Terfenol-D)-epoxy mixed components (MSCP) barium titanate and two phase MEE material. Here C_{ij} is expressed in $10^9 N/m^2$; e_{ij} in C/m^2 ; ϵ_{ij} in $10^{-9} C/Vm$; q_{ij} in N/Am ; μ_{ij} in $10^{-4} Ns^2/C^2$ and m_{ij} in $10^{-12} Ns/VC$.

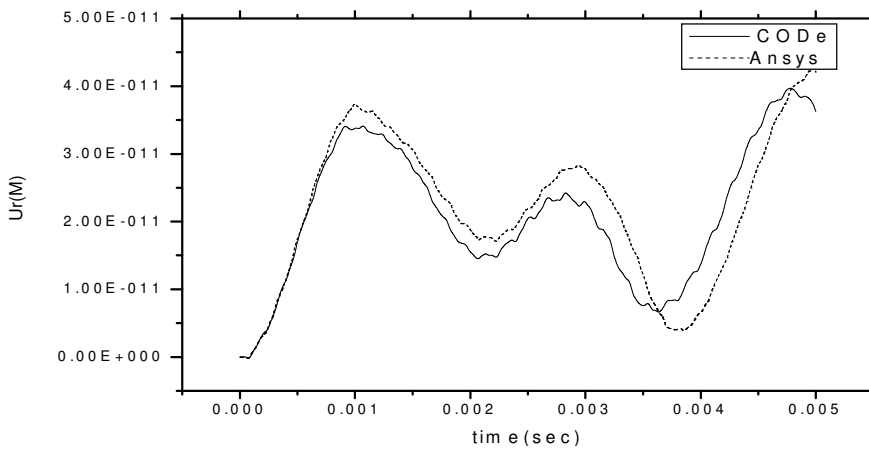


Figure 2. Comparison of U_r for PECP material.

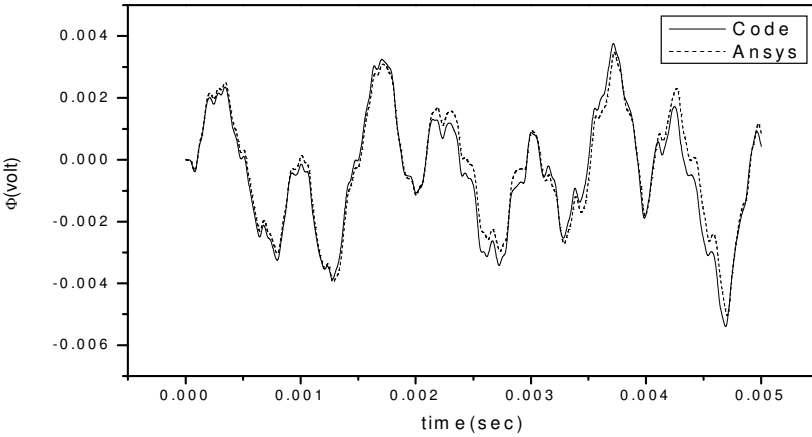


Figure 3. Comparison of ϕ for PECP material.

cylinder made of (PZT)-epoxy mixed component (PECP) and (Terfenol-D)-epoxy mixed components (MSCP) under simply supported boundary condition.

Ansys can directly solve the piezoelectric materials but the behavior of MSCP could not be computed directly with it. However, MSCP can be substituted by PECP; we note that the constitutive equations of both the materials are identical. The properties of the above material have been taken from [Liu et al. 2003]; see Table 1. The dimensions of the layered cylinder, length = 4 m, inner radius = 0.7 m and thickness = 0.6 m, are taken from [Wang and Zhong 2003]. The structure has been discretised with 6 elements in the radial direction and 40 elements in the axial direction. A constant internal pressure of 1 N/m^2 is applied. As is clear from Figures 2–5, the code results agree well with the Ansys results. The undulations in the curves of ϕ and ψ may be due to the presence of higher harmonics.

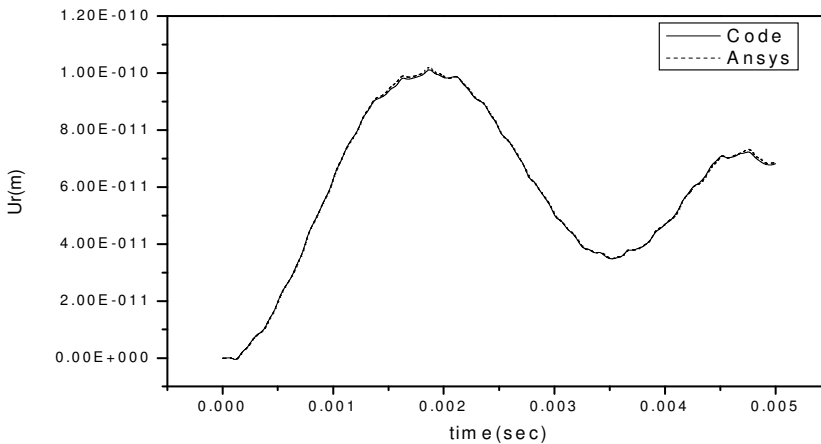


Figure 4. Comparison of U_r for MSCP Material.

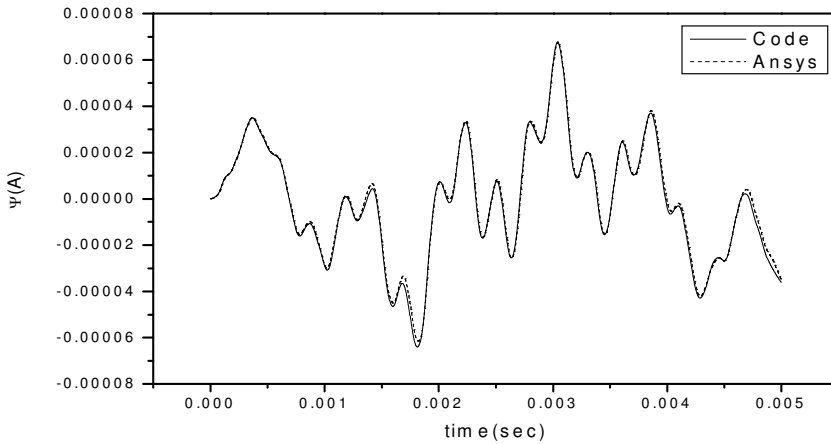


Figure 5. Comparison of ψ for MSCP Material.

| Materials | $V_m - 0.1$ | $V_m - 0.2$ | $V_m - 0.3$ | $V_m - 0.4$ | $V_m - 0.5$ |
|---------------------------|-------------|-------------|-------------|-------------|-------------|
| | $V_e - 0.5$ | $V_e - 0.4$ | $V_e - 0.3$ | $V_e - 0.2$ | $V_e - 0.1$ |
| C_{11} | 17.0 | 16.1 | 16.5 | 17.0 | 17.5 |
| C_{12} | 8.57 | 9.1 | 9.3 | 9.4 | 9.97 |
| C_{13} | 8.57 | 9.1 | 9.3 | 9.4 | 9.97 |
| C_{33} | 77.0 | 80.0 | 83.9 | 87.2 | 91.7 |
| C_{44} | 5.46 | 6.0 | 5.71 | 6.28 | 6.41 |
| C_{66} | 4.4 | 5.86 | 6.61 | 6.04 | 4.41 |
| e_{15} | 1.84 | 1.9 | 1.9 | 1.9 | 1.84 |
| e_{31} | 1.52 | 1.65 | 1.71 | 1.71 | 1.77 |
| e_{33} | 11.0 | 9.1 | 7.35 | 5.45 | 3.61 |
| ϵ_{11} | 0.394 | 0.294 | 0.264 | 0.235 | 0.205 |
| ϵ_{33} | 6.46 | 5.23 | 3.96 | 2.74 | 1.44 |
| μ_{11} | 2.92 | 3.15 | 2.92 | 3.14 | 3.37 |
| μ_{33} | 0.214 | 0.356 | 0.502 | 0.65 | 0.79 |
| q_{15} | 0.721 | 0.721 | 0.721 | 0.721 | 0.721 |
| q_{31} | 5.23 | 7.93 | 11.5 | 15.1 | 17.8 |
| q_{33} | 29.5 | 59.3 | 87.2 | 118.0 | 147.0 |
| $m_{11}(\times 10^{14})$ | 0.171 | 0.254 | 0.265 | 0.218 | 0.126 |
| $m_{33}(\times 10^{-10})$ | 0.658 | 1.03 | 1.18 | 1.03 | 0.652 |

Table 2. Material properties of the three-phase MEE materials for different volume fractions of the three-phase MEE material. Note that for all the materials the piezoelectric volume fraction (vf) is 0.4. Here V_m represents the piezomagnetic volume fraction and V_e represents the elastic matrix volume fraction. Also, C_{ij} is expressed in $10^9 N/m^2$; e_{ij} in C/m^2 ; ϵ_{ij} in $10^{-9} C/Vm$; q_{ij} in N/Am ; μ_{ij} in $10^{-4} Ns^2/C^2$ and m_{ij} in Ns/VC .

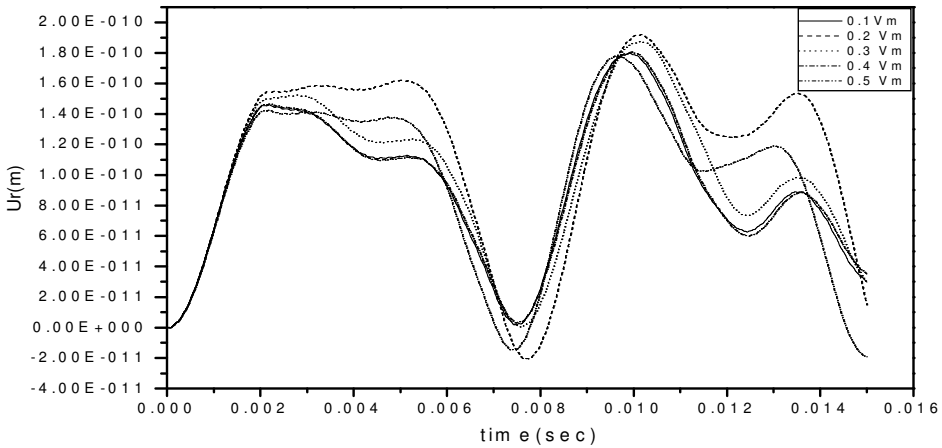


Figure 6. Comparison of U_r for different vf of MEE Material.

4.2. Response of the three-phase magneto-electro-elastic cylinder. The present computer code has been used to determine the response of three-phase magneto-electro-elastic layered cylinder under a constant internal pressure of 1 N/m^2 . The dimensions of the layered cylinder, length = 4 m, inner radius = 0.7 m and thickness = 0.6 m, are taken from [Wang and Zhong 2003]. The response has been studied at the middle node of the layered cylinder. The material properties are taken from [Jaesang et al. 2005] which are given in Table 2. In the MEE composite, the volume fraction of the fibrous piezoelectric phase is kept as constant 0.4 and the volume fraction of the piezomagnetic phase varies from 0.1–0.5; the remaining volume fraction is for the elastic material. The coupled response of the layered cylinder made of three phase magneto-electro-elastic material with a simply supported boundary condition has been plotted in Figures 10–13. The response has been plotted for a time period of 0.015 sec. In Figures 10–13, V_m represents the piezoelectric volume fraction.

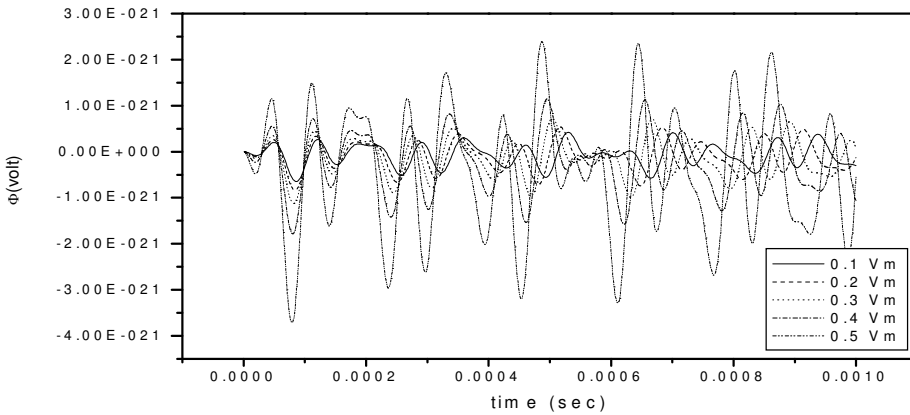


Figure 7. Comparison of ϕ for different vf of MEE material.

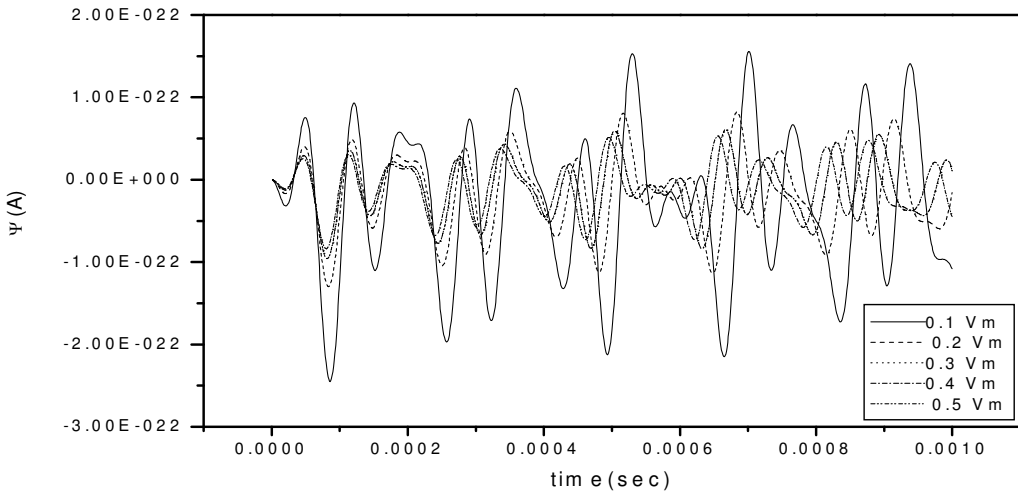


Figure 8. Comparison of ψ for different vf of MEE material.

Figure 6 shows the variation of radial displacement with respect to time. The variation of displacement for all the volume fraction more or less follows the same pattern. The peak value of the radial displacement occurs for the 0.2 volume fraction of the piezomagnetic fiber. The peak value of the displacement decreases with the increase in volume fraction of piezomagnetic phase in the MEE composite. This can be attributed to the fact that the stiffness of the cylinder increases with the increase in volume fraction of piezomagnetic phase as evident from the material properties given in Table 2.

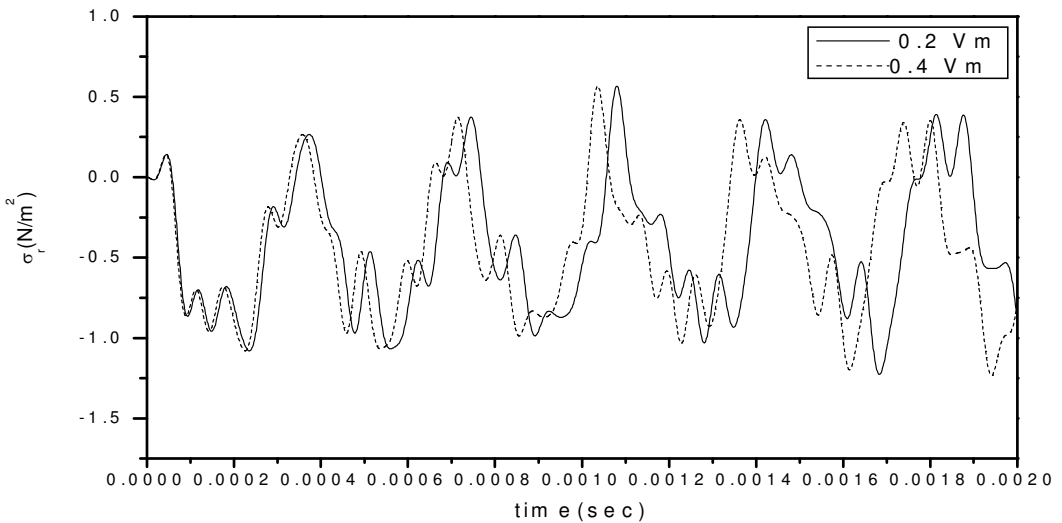


Figure 9. Comparison of σ_r for different vf of MEE material.

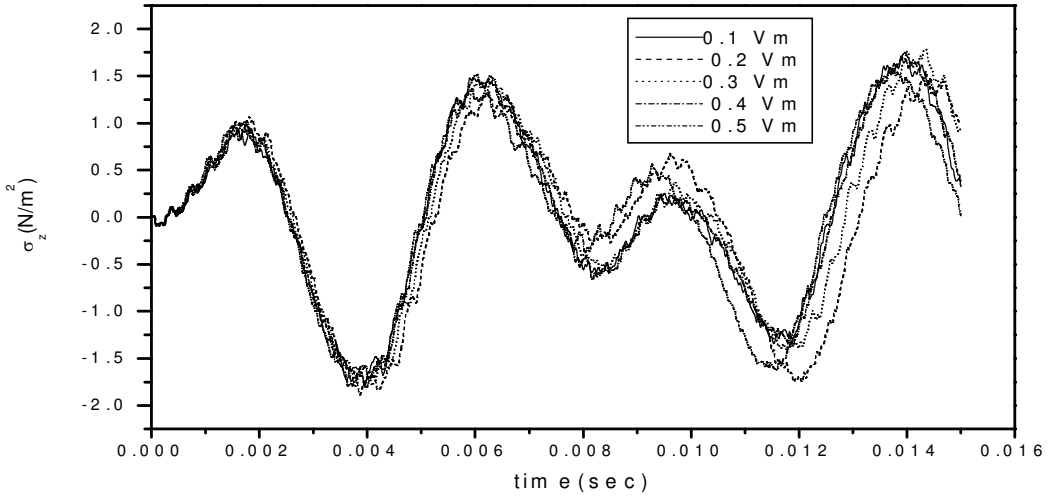


Figure 10. Comparison of σ_z for different vf of MEE material.

Figure 7 shows the magnified view of the variation of electric potential (ϕ) for different volume fractions for a time period of 0.001 sec. The distribution of ϕ shows the presence of higher harmonics. The value of ϕ reaches a maximum for the 0.5 volume fraction of the piezomagnetic fiber and it decreases with the decrease in volume fraction. The distribution of ϕ follows similar trend for all the materials.

Figure 8 shows the magnified view of the distribution of magnetic potential (ψ) for the different volume fractions of the piezomagnetic fiber for a time period of 0.001 sec. It is maximum for 0.1 volume fraction of the piezomagnetic fiber and goes on decreasing with the increase in volume fraction.

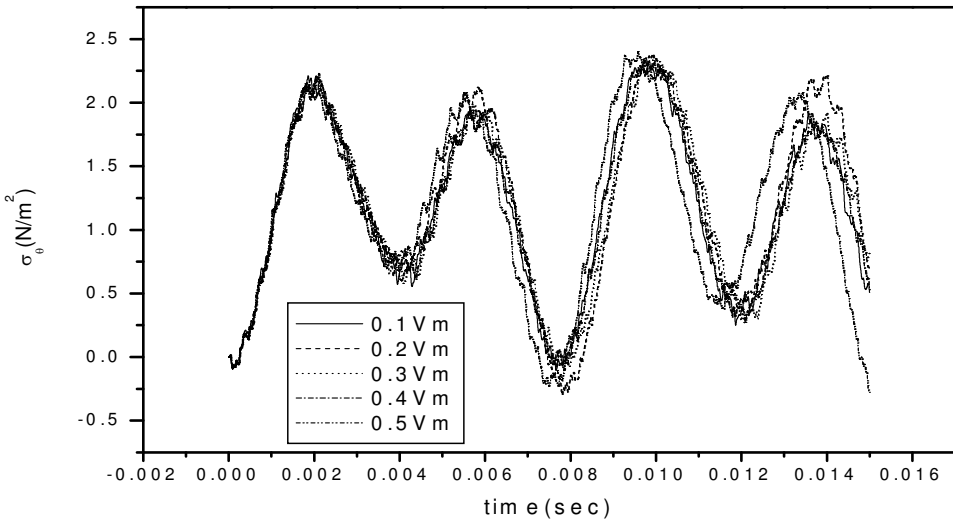


Figure 11. Comparison of σ_θ for different vf of MEE material.

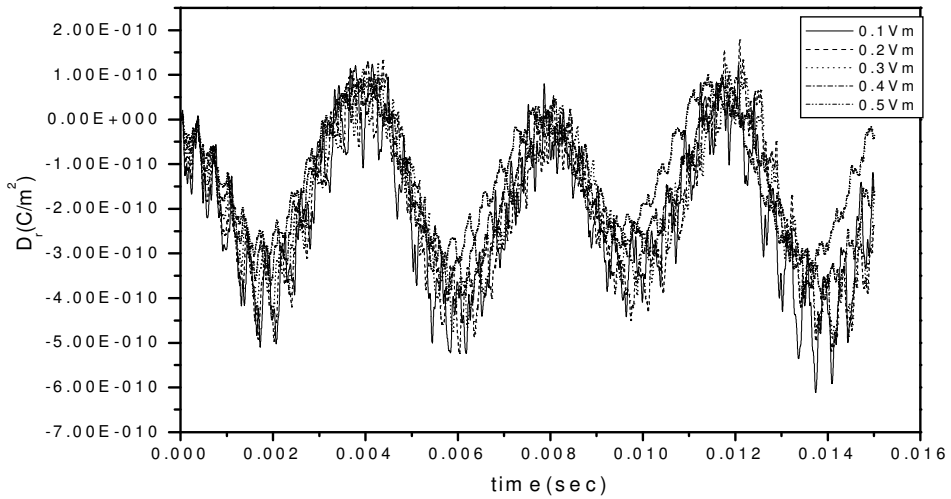


Figure 12. Comparison of D_r for different vf of MEE material.

Figures 9–11 show the distribution of stresses at the middle element of the layered cylinder. Figure 9 shows the magnified view of the distribution of radial stress (σ_r) for 0.2 and 0.4 volume fractions of the piezomagnetic fiber for a time period of 0.002 sec. The presence of higher harmonics can be seen from the stress distribution plots. The distribution of stress follows the same pattern for all volume fractions. The peak values of stresses are higher for σ_θ and σ_z compared to the other two, while σ_θ acts as a primary stress and its value is at a maximum for the 0.5 volume fraction of the piezomagnetic fiber.

Figure 12 shows the distribution of radial (D_r) electric displacement. The distribution pattern is similar for all the volume fractions of the MEE material. The value of the radial electric displacement

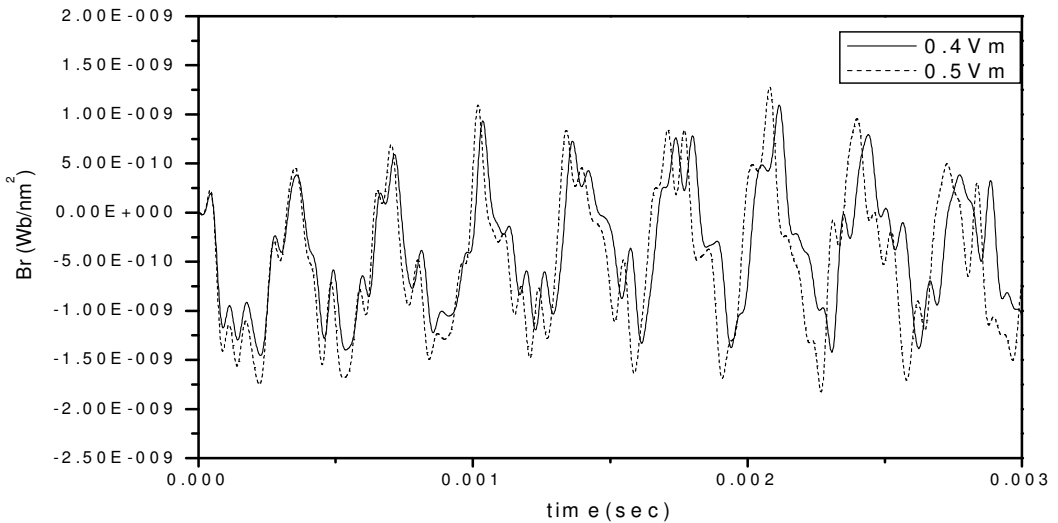


Figure 13. Comparison of B_r for different vf of MEE material.

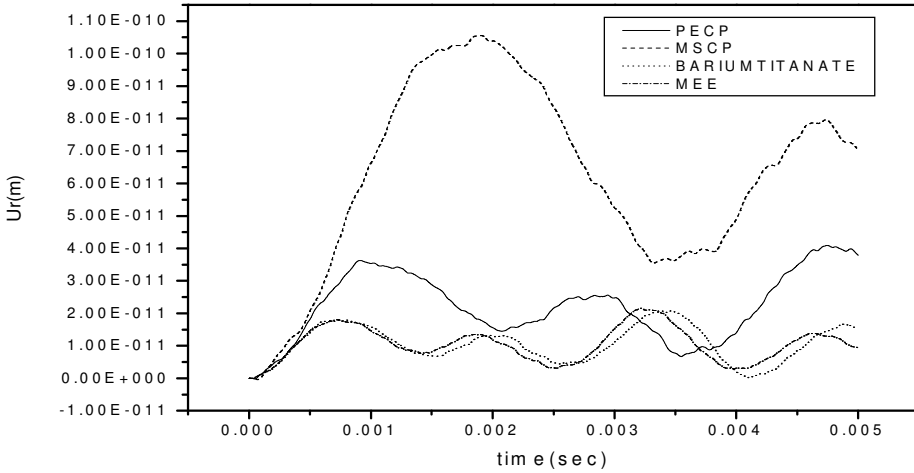


Figure 14. Comparison of U_r for simply supported layered cylinder.

is larger than that of the axial displacement. The peak value of D_r is for the 0.1 volume fraction of the piezomagnetic fiber and goes on decreasing with the increase in volume fraction. Figure 13 shows the magnified view of the distribution of radial magnetic induction (B_r) for the 0.4 and 0.5 volume fractions of the piezomagnetic fiber for a time period of 0.003 sec. The distribution pattern is similar for all the volume fractions of the piezomagnetic fiber in the MEE material. The value of the radial magnetic induction is larger than that of the axial magnetic induction. The peak value of B_r is for the 0.5 volume fraction of the piezomagnetic fiber and goes on decreasing with the decrease in volume fraction.

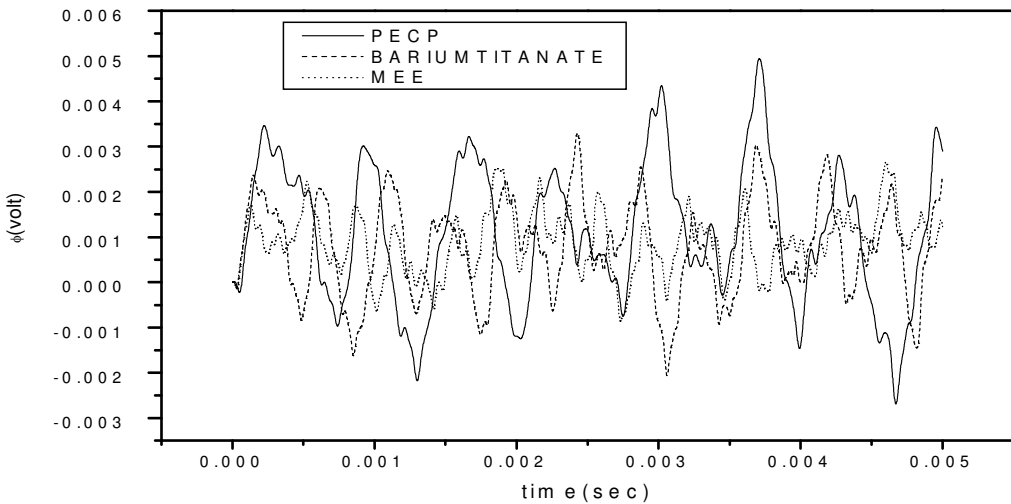


Figure 15. Comparison of ϕ for simply supported layered cylinder.

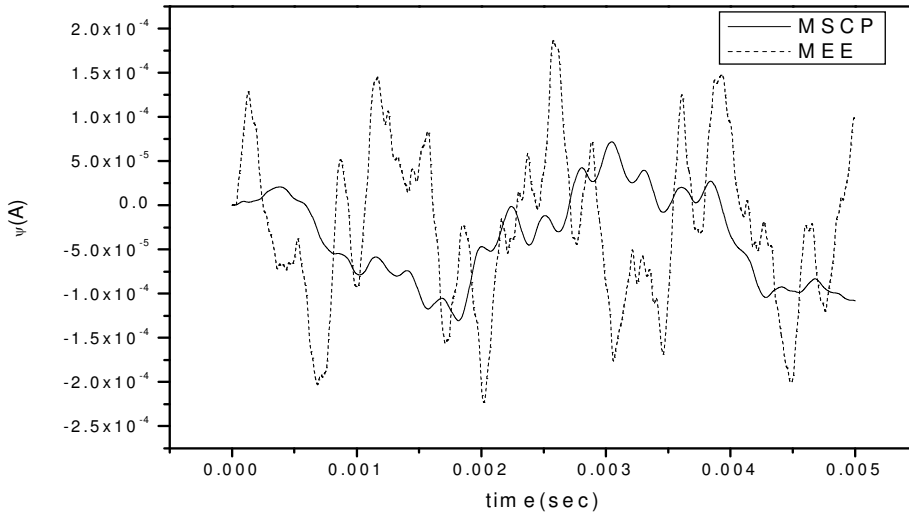


Figure 16. Comparison of ψ for simply supported layered cylinder.

4.3. Comparative studies of the responses of (PZT)-epoxy mixed component (PECP), (Terfenol-D)-epoxy mixed components (MSCP), barium titanate and a two phase MEE simply supported layered cylinder. The coupled response of the layered cylinder for different material with simply supported boundary conditions has been plotted in the Figures 14–16. The material properties for PECP and MSCP are taken from [Liu et al. 2003], barium titanate from [Aboudi 2001] and two phase MEE from [Jiang and Pan 2004]. The response at the middle node, that is, at the center of the layered cylinder, has been studied for a time lapse of 0.005 sec. Figure 14 shows that the peak value of the radial displacement U_r is maximum for the MSCP material and low for MEE material. This is due to the stiffening effect of the piezoelectric and piezomagnetic terms which increases the stiffness of the structure resulting from the generation of induced electric and magnetic fields in the MEE structures. It is clear from the displacement plot that the frequency is lowest for MSCP material and highest for MEE and BaTiO₃.

Figure 15 shows the variation of electric potential (ϕ) for the materials exhibiting piezoelectric characteristics. The value of electric potential (ϕ) is highest for PECP material and low for MEE material, which can be attributed to Equation (13) that the value of ϕ is directly proportional to displacement, which is also high for PECP material. The distribution of ϕ for all the materials follows the same pattern. Figure 16 shows the distribution of ψ for the materials exhibiting piezomagnetic characteristics. The value of ψ is larger for MEE material, and is due to the presence of high piezomagnetic coefficients compared to MSCP material given in Table 1.

The distribution of stresses at the middle element of the layered cylinder for all the materials is studied using the Equation (1). The peak values of σ_θ are high compared to other stresses. The value of stresses is maximum for MEE material. The stress distribution also reveals the presence of higher harmonics in the response. The distribution of the radial (D_r) and axial (D_z) electric displacement at the middle element of the layered cylinder for all the materials is studied using the Equation (2). The value of electric displacement in the radial direction is greater than that in the axial direction. The magnitude of

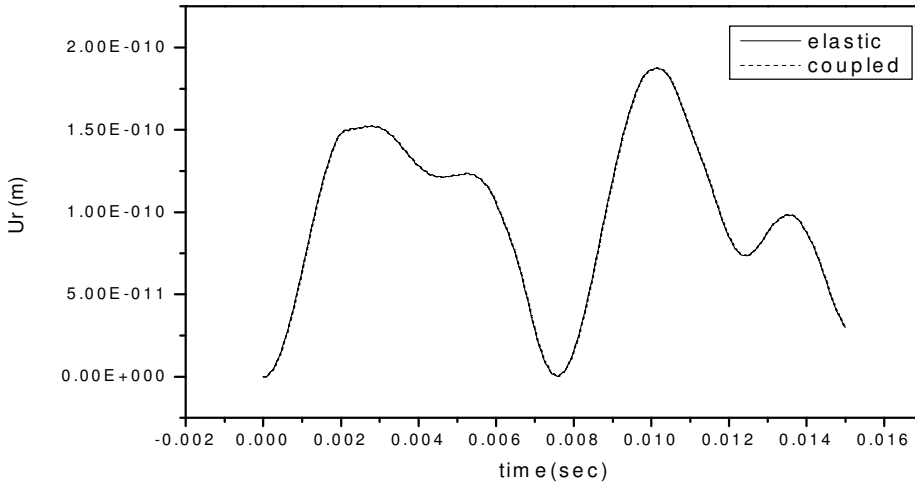


Figure 17. Comparison of U_r for elastic and coupled response for MEE material.

electric displacement is at its maximum for a cylinder made of PECP material, and is at a minimum for a cylinder made of MEE material—a fact which can be due to the presence of piezomagnetic coupling terms present in the MEE material. The distribution of radial (Br) and axial (Bz) magnetic induction at the middle element of the layered cylinder for all the materials is studied using the Equation (3). The value of magnetic induction in the radial direction is larger than that in the axial direction and is a maximum for MEE structures.

4.4. Comparison between the elastic and coupled responses of three phase magneto-electro-elastic simply supported layered cylinder. A comparison between the elastic and the coupled responses for the three phase magneto-electro-elastic simply supported layered cylinder has been plotted in Figure 17. The comparison of response is done for 0.3 vf of the piezomagnetic phase in the MEE composite. From the figure it is clear that the piezoelectric and piezomagnetic coupling terms do not play a part in the response of three phase magneto-electro-elastic structures. The contribution of coupling coefficients is negligible in the stiffness matrix of the structure. Hence the distribution of coupled ϕ and ψ is similar to that of uncoupled (elastic) ϕ and ψ .

5. Conclusion

The finite element method has been used to find the transient response of the three-phase magneto-electro-elastic simply supported layered cylinder under constant internal pressure. Numerical results have been presented for different volume fractions of the piezomagnetic phase in the composite. The responses of purely piezoelectric and piezomagnetic phases can also be calculated as special cases. A comparative study of the response of PECP, MSCP, barium titanate and two phase magneto-electro-elastic materials has been presented. A comparison between the coupled and the elastic responses of the 0.3 volume fraction of the three phase magneto-electro-elastic structure is also presented. It can be concluded from this study that (i) the magnitude of displacement is high for the three-phase MEE materials as compared with the other materials; (ii) the transient responses of the three-phase materials

show more complex characteristics compared with the other materials presented in the paper; (iii) the piezoelectric and piezomagnetic coupling terms do not play a role in the transient response of three-phase magneto-electro-elastic structures; and (iv) the magnitudes of electric potential and magnetic potential are low for the three-phase materials compared with the other materials which can be attributed to the low values of piezoelectric and piezomagnetic coefficients in the three-phase material.

References

- [Aboudi 2001] J. Aboudi, "Micromechanical analysis of fully coupled electro-magneto-thermo-elastic multiphase composites", *Smart Mater. Struct.* **10** (2001), 867–877.
- [Annigeri et al. 2006] A. R. Annigeri, N. Ganesan, and S. Swarnamani, "Free vibration of clamped clamped magneto-electro-elastic cylinder shell", *J. Sound Vib.* **292** (2006), 300–314.
- [Bhangale and Ganesan 2005] R. K. Bhangale and N. Ganesan, "Free vibration studies of simply supported non-homogeneous functionally graded magneto-electro-elastic finite cylindrical shells", *J. Sound Vib.* **288** (2005), 412–422.
- [Bhimaraddi 1987] A. Bhimaraddi, "Static and transient response of cylindrical shells", *Thin Walled Structures* **5** (1987), 157–179.
- [Buchanan 2003] G. R. Buchanan, "Free vibration of an infinite magneto-electro-elastic cylinder", *J. Sound Vib.* **268** (2003), 413–426.
- [Hou and Leung 2004] P. F. Hou and A. Y. T. Leung, "The transient responses of magneto-electro-elastic hollow cylinders", *Smart Mater. Struct.* **13** (2004), 762–776.
- [Jaesang et al. 2005] L. Jaesang, G. James, I. V. Boyd, and C. L. Dimitris, "Effective properties of three-phase electro-magneto-elastic composites", *Int. J. Eng. Sci.* **43** (2005), 790–825.
- [Jiang and Pan 2004] X. Jiang and E. Pan, "Exact solution of the 2D polynomoal inclusion problem in anisotropic magneto-electroelastic full-, half-, and bilateral-planes", *Int. J. Solids Struct.* **41**:16–17 (2004), 4361–4382.
- [Liu et al. 2003] Y. X. Liu, J. G. Wan, J. M. Liu, and C. W. Nan, "Effect of magnetic bias field on magnetoelectric coupling in magnetoelectric composites", *J. Appl. Phys.* **94** (2003), 5118–5122.
- [Pan and Heyliger 2002] E. Pan and P. R. Heyliger, "Free vibrations of simply supported and multilayered magneto-electro-elastic plates", *J. Sound Vib.* **252** (2002), 429–442.
- [Philip 1972] U. Philip, "Transient response of inelastic shells of revolution", *Comput. Struct.* **2** (1972), 975–989.
- [Wang and Zhong 2003] X. Wang and Z. Zhong, "A finitely long circular cylindrical shell of piezoelectric/piezomagnetic composite under pressuring and temperature change", *Int. J. Eng. Sci.* **41** (2003), 2429–2445.

Received 8 May 2007. Accepted 1 Aug 2007.

ATUL DAGA: atul_daga@rediffmail.com

Machine Design Section, Indian Institute of Technology Madras, Chennai 600 036, India

NATRAJAN GANESAN: nganesan@iitm.ac.in

Department of Mechanical Engineering, Indian Institute of Technology Madras, Chennai 600 036, India

KRISHNAPILLAI SHANKAR: skris@iitm.ac.in

Department of Mechanical Engineering, Indian Institute of Technology Madras, Chennai 600 036, India

